

Improving Solid-State NMR Dipolar Recoupling by Optimal Control

Cindie T. Kehlet,^{†,‡} Astrid C. Sivertsen,[†] Morten Bjerring,[†] Timo O. Reiss,[‡] Navin Khaneja,^{||}
Steffen J. Glaser,[‡] and Niels Chr. Nielsen^{*,†}

Interdisciplinary Nanoscience Center (iNANO) and Laboratory for Biomolecular NMR Spectroscopy, Department of Chemistry, University of Aarhus, DK-8000 Aarhus C, Denmark, Institut für Organische Chemie und Biochemie, Technische Universität München, D-85747 Garching, Germany, and Division of Applied Sciences, Harvard University, Cambridge, Massachusetts 02138

Received March 3, 2004; E-mail: ncn@chem.au.dk

The past few years have witnessed considerable progress in solid-state NMR toward atomic-resolution structural analysis of biological macromolecules.¹ This is relevant for membrane proteins, protein assemblies, and enzyme–substrate complexes not earlier amenable for structural analysis because of low molecular tumbling or lack of suitable crystals. A key factor in the progress of solid-state NMR is the development of methods that enable the achievement of high-resolution spectra with detailed structural information. Among different approaches, the combination of magic-angle-spinning (MAS) with radio frequency (rf) irradiation for selective reintroduction of dipole–dipole interactions has proven to be particularly useful. Experiments “recoupling” specific homo-^{2–5} or heteronuclear^{6–10} dipolar couplings enable transfer of magnetization from atom to atom in the molecule to provide protocols for spectral assignment similar to those used in liquid-state NMR.¹¹ Likewise, dipolar recoupling is fundamental in establishing structural constraints in terms of internuclear distances¹² and torsion angles.¹³

The success of biological solid-state NMR critically depends on the performance of the recoupling methods used as building blocks in the multiple-dimensional experiments. They have to provide the most efficient transfer within the shortest possible time while being sufficiently specific that loss of coherence by transfer to undesired spins is avoided. With these criteria, a large number of recoupling methods have been designed, typically based on intuition and analytical tools such as effective Hamiltonian theory.¹⁴ Alternatives, such as numerical¹⁵ and experimental search for experiments,¹⁶ have been more sparse.

In this Communication, we describe for the first time application of optimal control theory¹⁷ for systematic design of solid-state NMR experiments. Optimal control theory, taking its origin in economy and engineering, have previously been used for optimizing experiments in coherent optics,¹⁸ magnetic resonance imaging,¹⁹ and liquid-state NMR.²⁰ Here it is applied for the development of solid-state NMR dipolar recoupling experiments, where the challenge is to minimize the loss of signal due to crystallite-orientation dependencies while coping with effects from anisotropic shielding, desires regarding operative chemical shift ranges, and instrumental imperfections. Consideration of these effects is difficult by analytical means, implying that we here explore a setup with integration of optimal control theory and numerical simulations using SIMPSON.²¹ In this manner, it is possible to exploit all experimental degrees of freedom and undertake the formidable task of optimizing experiments in terms of thousands of control variables being amplitudes and phases of irradiation on two rf channels in small steps over the desired excitation period.

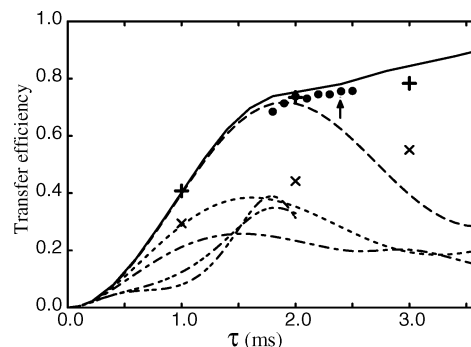


Figure 1. ¹⁵N to ¹³C^α coherence transfer efficiencies calculated for a powder of glycine (400 MHz for ¹H, $\delta_{\text{aniso}}(^{15}\text{N}) = 10.1$ ppm, $\eta_{\text{N}} = 0.17$, $\delta_{\text{aniso}}(^{13}\text{C}) = 19.4$ ppm, $\eta_{\text{C}} = 0.98$, $b_{\text{NC}}/2\pi = 890$ Hz) with 10 kHz MAS. Efficiencies for optimal control sequences (solid) and DCP under homogeneous (---) as well as 5% (···) and 10% (-·-·-) Lorentzian inhomogeneous rf fields (percentage reflects full width of the rf profile at half-height relative to the nominal rf field strength). For DCP, the nominal rf field strengths were $\omega_{\text{rf,N}}/2\pi = 35$ kHz and $\omega_{\text{rf,C}}/2\pi = 25$ kHz. For comparison, we included efficiencies for DCP with a 10% linear ramp of $\omega_{\text{rf,C}}/2\pi$ (around 25 kHz) from 0 to 2 ms using ideal (···) and 5% Lorentzian inhomogeneous (····) rf fields, as well as numerically optimized adiabatic-passage CP experiments using $\omega_{\text{rf,N}}/2\pi(^{15}\text{N}) = 37$ kHz and a tangential sweep around 47 kHz on ¹³C without (+) and with 5% Lorentzian inhomogeneity (x). Solid circles refer to ¹³CDCP experiments optimized under inhomogeneous rf fields.

Taking ¹⁵N to ¹³C^α coherence transfer in a powder of ¹³C_α, ¹⁵N-labeled glycine spinning at 10 kHz as an example, Figure 1 shows calculated transfer efficiencies achievable by optimal control experiments along with efficiencies for double-cross-polarization (DCP)⁶ and adiabatic-passage cross-polarization (AP-CP)¹⁰ experiments. DCP is the most frequently used experiment for ¹⁵N to ¹³C coherence transfers, and with the present relatively small chemical shielding anisotropies it is among the most efficient experiments for this purpose. The optimal control sequences were calculated by digitizing the rf irradiation in steps of 5 μs and setting upper limits of 33 and 37 kHz on the ¹⁵N and ¹³C rf field strengths, respectively. It is clear from Figure 1 that optimal control provides a means to obtain larger transfer efficiencies than the 72% offered by DCP, indicating a more efficient elimination of the crystallite orientation dependency than γ -encoding³ at transfer times shorter than typically recommended for AP-CP.¹⁰ This is remarkable, but it is obviously also of interest to consider the performance of DCP, linearly ramped DCP, AP-CP, and optimal control sequences in the presence of inhomogeneous rf fields. In typical cases, the efficiency of DCP and AP-CP is reduced by more than 30–50% as illustrated in Figure 1. For comparison, Figure 1 includes points representative for optimal control DCP (¹³CDCP) experiments optimized under the assumption of 5% Lorentzian (matched the inhomogeneity in our probe slightly better than a 9.2% Gaussian

[†] University of Aarhus.

[‡] Technische Universität München.

^{||} Harvard University.

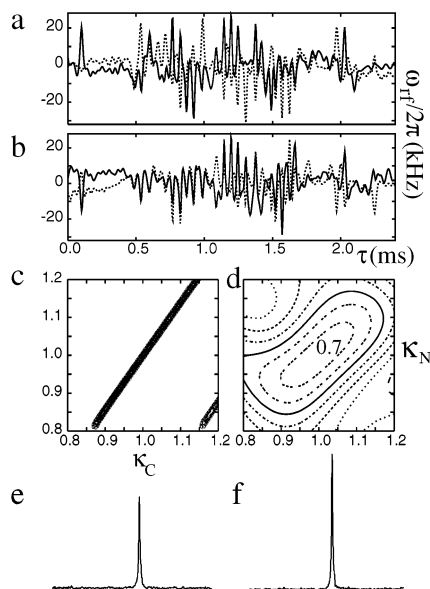


Figure 2. (a) ^{15}N and (b) ^{13}C rf amplitudes²² for the 2.4 ms $^{\text{O}}\text{DCP}$ sequence marked with an arrow in Figure 1. Solid/dotted lines refer to x -/ y -rf phase. Rf field dependencies (in terms of scale factor κ_{N} and κ_{C} on the nominal rf field strength) for (c) DCP and (d) $^{\text{O}}\text{DCP}$ (contours separated by 0.1, solid line 0.5 efficiency). Experimental (e) DCP and (f) $^{\text{O}}\text{DCP}$ spectra for a powder of $^{13}\text{C}\alpha,^{15}\text{N}$ -glycine using 10 kHz spinning. The experiments used ^1H decoupling in excess of 100 kHz.

profile) or more severe rf inhomogeneity. It appears that the efficiency may be improved by 50–100% using $^{\text{O}}\text{DCP}$ instead of DCP or AP-CP.

Figure 2a,b shows rf pulse shapes for a 2.4 ms $^{\text{O}}\text{DCP}$ experiment optimized from a random pulse sequence using SIMPSON with optimal control implemented in a conjugated gradient approach. The sequence in Figure 2a,b has root-mean-square average rf field strengths of 10.4 and 9.5 kHz on the ^{15}N and ^{13}C channels, which compares very favorably with the 35 and 25 kHz used for DCP, and even better for AP-CP, considering that rf heating is a major problem in biological solid-state NMR. Figures 2c,d show the rf field dependencies of the transfer efficiencies for DCP and the $^{\text{O}}\text{DCP}$ experiment in Figure 2a,b. These plots reveal that the high sensitivity of DCP toward rf inhomogeneity may efficiently be removed using $^{\text{O}}\text{DCP}$. We note that $^{\text{O}}\text{DCP}$ can be optimized to the same efficiency with a much broader inhomogeneity profile, implying that the actual profile is not as critical for $^{\text{O}}\text{DCP}$ as it is for DCP and AP-CP; it is just a matter of optimizing the experiment to a profile that at least is as severe as that of the probe. We also note that the $^{\text{O}}\text{DCP}$ sequences represented here display chemical shift offset profiles similar to those of DCP, but we envisage that consideration of specific offsets and anisotropy profiles in the optimization may provide $^{\text{O}}\text{DCP}$ experiments with good performance for essentially any offset profile.

Various $^{\text{O}}\text{DCP}$ experiments were tested experimentally on $^{13}\text{C}\alpha,^{15}\text{N}$ -labeled glycine using a 400 MHz Bruker Avance NMR spectrometer with a 4 mm triple-resonance probe. The rf pulse shapes were implemented as the $^{15}\text{N} \rightarrow ^{13}\text{C}$ element in a $^1\text{H} \rightarrow ^{15}\text{N} \rightarrow ^{13}\text{C}$ triple-resonance experiment, leading to the experimental spectrum in Figure 2f. For comparison, Figure 2e shows the corresponding spectrum recorded using DCP. In the present case, $^{\text{O}}\text{DCP}$ improves the coherence transfer by 53% relative to DCP. In cases of larger sample volumes, and thereby larger rf inhomogeneity, the gain may be higher.

In conclusion, we have presented the first use of optimal control theory for the design of solid-state NMR experiments. Our work

demonstrates that substantial improvements of typical experiments may readily be obtained. It is foreseen that similar gains may be obtained for many of the building blocks used in current solid-state NMR experiments. Thus, the optimal control approach presented in this paper may have a substantial impact on the next generations of solid-state NMR experiments in applications ranging from materials science to biology.

Acknowledgment. This work has been supported by the Danish Biotechnological Instrument Center, Carlsbergfondet, The Danish Natural Science Foundation, and by the Deutsche Forschungsgemeinschaft (GI 203/4-2).

References

- (1) McDermott, A. E.; Polenova, T.; Böckmann, A.; Zilm, K. W.; Martin, R. W.; Montelione, G. T.; Paulsen, E. K. *J. Biomol. NMR* **2000**, *16*, 459.
- (2) Castellani, J.; van Rossum, B.; Diehl, A.; Schubert, M.; Rehbein, K.; Oschkinat, H. *Nature* **2002**, *420*, 98.
- (3) Böckmann, A.; Lange, A.; Galinier, A.; Luca, S.; Giraud, N.; Juy, M.; Heise, H.; Monstserret, R.; Penin, F.; Baldus, M. *J. Biomol. NMR* **2003**, *27*, 323.
- (4) Jaroniec, C. P.; MacPhee, C. E.; Baja, V. S.; McMahon, M. T.; Dobson, C. M.; Griffin, R. G. *Proc. Natl. Acad. Sci. U.S.A.* **2004**, *101*, 711.
- (5) Tycko, R.; Dabaghi, G. *Chem. Phys. Lett.* **1990**, *173*, 461.
- (6) Nielsen, N. C.; Bildsøe, H.; Jakobsen, H. J.; Levitt, M. H. *J. Chem. Phys.* **1994**, *101*, 1805.
- (7) Lee, Y. K.; Kurur, N. D.; Helmle, M.; Johannesen, O.; Nielsen, N. C. *Chem. Phys. Lett.* **1995**, *242*, 304.
- (8) Hohwy, M.; Jakobsen, H. J.; Edén, M.; Levitt, M. H.; Nielsen, N. C. *J. Chem. Phys.* **1998**, *108*, 2686.
- (9) Verel, R.; Baldus, M.; Nijman, M.; van Os, J. W. M.; Meier, B. H. *Chem. Phys. Lett.* **1997**, *280*, 31.
- (10) Schaefer, J.; Stejskal, E. O.; Garbow, J. R.; McKay, R. A. *J. Magn. Reson.* **1984**, *59*, 150.
- (11) Gullion, T.; Schaefer, J. *Adv. Magn. Reson.* **1989**, *13*, 55.
- (12) Sun, B. Q.; Costa, P. R.; Griffin, R. G. *J. Magn. Reson. A* **1995**, *112*, 191.
- (13) Brinkman, A.; Levitt, M. H. *J. Chem. Phys.* **2001**, *115*, 357.
- (14) Baldus, M.; Geurts, D. G.; Hediger, S.; Meier, B. H. *J. Magn. Reson. A* **1996**, *118*, 140.
- (15) Cavanagh, J.; Fairbrother, W. J.; Palmer, A. G., III; Skelton, N. J. *Protein NMR Spectroscopy. Principles and Practice*; Academic Press: San Diego, 1996.
- (16) Holl, S. M.; Marshall, G. R.; Beusen, D. D.; Kociolek, K.; Redlinski, A. S.; Leplawy, M. T.; McKay, R. A.; Vega, S.; Schaefer, J. *J. Am. Chem. Soc.* **1992**, *114*, 4830.
- (17) Verdegem, P. J. E.; Helmle, M.; Lugtenburg, J.; de Groot, H. J. M. *J. Am. Chem. Soc.* **1997**, *119*, 169.
- (18) Jaroniec, C. P.; Toung, B. A.; Rienstra, C. M.; Herzfeld, J.; Griffin, R. G. *J. Am. Chem. Soc.* **1999**, *121*, 10237.
- (19) Ishii, Y.; Terao, T.; Kainosho *Chem. Phys. Lett.* **1996**, *256*, 133.
- (20) Feng, X.; Lee, Y. K.; Sandström, D.; Edén, M.; Maisel, H.; Sebald, A.; Levitt, M. H. *Chem. Phys. Lett.* **1996**, *257*, 314.
- (21) Hong, M.; Gross, J. D.; Griffin, R. G. *J. Phys. B* **1997**, *101*, 5869.
- (22) Haberland, U.; Waugh, J. S. *Phys. Rev.* **1968**, *175*, 453.
- (23) Hohwy, M.; Nielsen, N. C. *J. Chem. Phys.* **1998**, *109*, 3780.
- (24) Untidt, T. S.; Nielsen, N. C. *Phys. Rev. E* **2002**, *65*, 021108.
- (25) Liu, H.; Glaser, S. J.; Drobny, G. P. *J. Chem. Phys.* **1990**, *93*, 7543.
- (26) Sakellariou, D.; Lesage, A.; Hodgkinson, P.; Emsley, L. *Chem. Phys. Lett.* **2000**, *319*, 253.
- (27) De Paepe, G.; Giraud, N.; Lesage, A.; Hodgkinson, P.; Böckmann, A.; Emsley, L. *J. Am. Chem. Soc.* **2003**, *125*, 13938.
- (28) Pontryagin, L.; Boltyanskii, B.; Gamkrelidze, R.; Mishchenko, E. *The Mathematical Theory of Optimal Processes*; Wiley-Interscience: New York, 1962.
- (29) Bryson, A., Jr.; Ho, Y.-C. *Applied Optimal Control*; Hemisphere: Washington, DC, 1975.
- (30) Peirce, A. P.; Dahleh, M. A.; Rabitz, H. *Phys. Rev. A* **1988**, *37*, 4950.
- (31) Conolly, S.; Nishimura, D.; Macovski, A. *IEEE Trans. Med. Imag.* **1986**, *MI-5*, 106.
- (32) Rosenfeld, D.; Zur, Y. *Magn. Res. Med.* **1996**, *36*, 401.
- (33) Reiss, T.; Khaneja, N.; Glaser, S. J. *J. Magn. Reson.* **2002**, *154*, 192.
- (34) Khaneja, N.; Reiss, T.; Luy, B.; Glaser, S. J. *J. Magn. Reson.* **2003**, *162*, 311.
- (35) Skinner, T. E.; Reiss, T. O.; Luy, B.; Khaneja, N.; Glaser, S. J. *J. Magn. Reson.* **2003**, *163*, 8.
- (36) Bak, M.; Rasmussen, J. T.; Nielsen, N. C. *J. Magn. Reson.* **2000**, *147*, 296.
- (37) Open source software: <http://bionmr.chem.au.dk>, accessed June, 2003.
- (38) Pulse sequence waveforms available at <http://bionmr.chem.au.dk>, accessed June, 2003.

JA048786E